

## Oxidative Coupling of Methane over Amorphous Lanthanum Aluminum Oxides

HISAO IMAI, TOMOHIKO TAGAWA, AND NAOKI KAMIDE

*Research Laboratory of Engineering Materials, Tokyo Institute of Technology, Midori-ku, Yokohama-shi, 227, Japan*

Received January 26, 1987; revised March 31, 1987

The oxidative coupling of methane was studied on a series of amorphous lanthanum aluminum oxides prepared by the mist decomposition method. The  $C_2$  activity was increased with increasing aluminum content, showing a maximum at 10 at.%. The  $C_2$  selectivity of 47% and total methane conversion of 25% was obtained at 983 K on this catalyst. A study on the effect of pretreatment temperature revealed that the active samples were amorphous and that the growth of the crystalline phases decreased greatly the  $C_2$  activity. The IR study indicated that octahedrally coordinated isolated aluminum ions, which were dispersed into the amorphous lanthanum oxide, constituted the active sites of the reaction. The two kinds of  $O_2$  adsorption sites were observed in the mixed oxides pretreated at 983 K. The study on the TPD spectra of a series of catalysts suggested that these sites were responsible for the oxidative coupling of methane. © 1987 Academic Press, Inc.

### INTRODUCTION

The oxidative coupling of methane is one of the most important reactions in relation to the chemical utilization of natural gas. Although many studies have been made to find an efficient catalyst under a variety of reaction conditions (1–16), it has not been possible to achieve both high activity and good selectivity for  $C_2$  hydrocarbon formation. Our recent communication (9) has demonstrated that the  $LaAlO_3$ , prepared by the mist decomposition method, shows a high activity for  $C_2$  hydrocarbon formation in an atmospheric flow reactor under a high oxygen partial pressure. As the mutual acceleration effect of lanthanum and aluminum was large in developing the  $C_2$  activity, a series of lanthanum aluminum oxides was prepared and some properties as well as the catalytic activities were measured to determine the active sites of the reaction.

### METHODS

Catalysts were prepared by the mist decomposition method (17, 18). A mist of a

mixed solution (5 wt%) of lanthanum nitrate and aluminum nitrate was produced by supersonic atomization and treated successively through three furnaces at the flow rate of 1 liter/min. The temperatures of the furnaces were maintained at 443, 573, and 1073 K, respectively, in this study. The fine particles of the mixed oxides were collected by a glass filter at 390 K. It should be noted that the retention time of the mist in the constant temperature portion ( $\pm 5$  K) of the furnaces was ca. 10 s. Lanthanum nitrate ( $>99.9\%$ ) was obtained from Soekawa Chemical Co., Ltd., while aluminum nitrate ( $>99.99\%$ ) was obtained from Wako Pure Chemical Industries, Ltd. The collected powders were dried overnight at 383 K, pressed into tablets, crushed, sized (32–60 mesh), and stored for use in the measurements.

The catalytic activities were measured by a flow method with the quartz reactor shown in Fig. 1. Methane and air were preheated separately in a two-fluid nozzle (20 mm o.d.; 100 mm long) and mixed rapidly just before the catalyst bed (14 mm i.d.). An inner cooler (10-mm-o.d. air

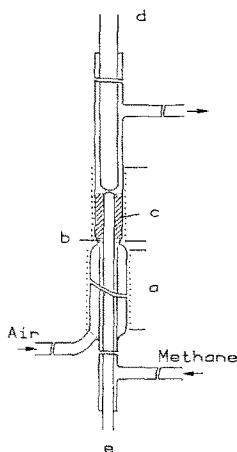


FIG. 1. Schematic diagram of the reactor: (a) preheater nozzle, (b) silica wool, (c) catalyst, (d) inner cooler, (e) thermocouple well.

cooler) was provided immediately after the catalyst bed for the rapid cooling of the exit gas. The difference in temperatures between the top and the bottom of the catalyst bed was kept within 2 K by independent control of the temperatures of the preheater nozzle and the catalyst bed. A constant volume (0.3 ml) of catalyst was diluted to 1.2 ml with quartz powder (32–60 mesh) and packed into the reactor. After pretreatment by air at 983 K for 16 h, 20 ml/min (at room temperature) of methane and 20 ml/min (at room temperature) of air were passed into the reactor at various temperatures. The reaction products were analyzed by a gas chromatography with 2m-Molecular Sieve 13X and 2m-Porapak Q columns. Methane (Research Grade, >99.95%) was obtained from Takachiho Chemical Co., Ltd., and fed to the reactor through a Molecular Sieve 3A column. Air was purified through sodium hydroxide solution and sulfuric acid successively.

In temperature-programmed desorption (TPD) studies, a constant weight (0.58 g) of catalyst was packed in a quartz measuring tube (8 mm o.d., 6 mm i.d.). After pretreatment by the purified air at 983 K for 16 h, the temperature of the catalyst was lowered to 323 K and kept constant for 30 min in the stream of the air. Then, 20 ml/min of

helium gas was passed through the measuring tube by a gas handling valve, and after 10 min the temperature of the catalyst was increased at the rate of 6.25 K/min. The composition of exit gas was monitored by a thermal conductivity cell at 373 K. A gas sampler was provided immediately after the cell for the detailed analysis of the desorbed gas. The analysis was made by gas chromatography with 0.6m-Molecular Sieve 5A and 0.5m-Porapak Q columns. Helium gas was obtained by Kayama Oxygen Co., Ltd., and purified through a Molecular Sieve 5A column and a rare gas purifier (Model RT-3, Japan Pure Hydrogen Co., Inc.), successively.

The specific surface areas were measured by the BET method from the adsorption of nitrogen at liquid nitrogen temperature. A Rigaku Denki powder X-ray diffractometer with nickel filtered  $\text{CuK}\alpha$  radiation, a Hitachi HSM2 scanning electron microscope, a Hitachi 295 infrared (IR) spectrometer, and a Shimadzu SA-CP3 particle size distribution analyzer were used for the characterization of the catalysts.

## RESULTS AND DISCUSSION

Figure 2 shows the surface areas of the catalysts pretreated at 983 K for 16 h. The surface areas are about  $2 \text{ m}^2/\text{g}$  except  $\text{La}_2\text{O}_3$  and  $\text{Al}_2\text{O}_3$ . Samples consisted of spherical particles as shown in Fig. 3. The particle size distribution measurement on  $\text{LaAlO}_3$  (aluminum content = 50 at.%) gave the average diameter of  $0.61 \mu\text{m}$  and the cumu-

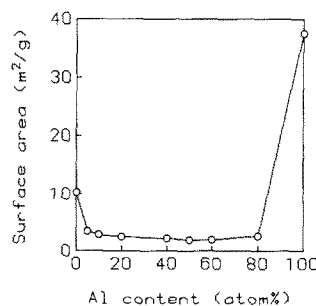


FIG. 2. Surface areas of catalysts. Pretreated at 983 K for 16 h.

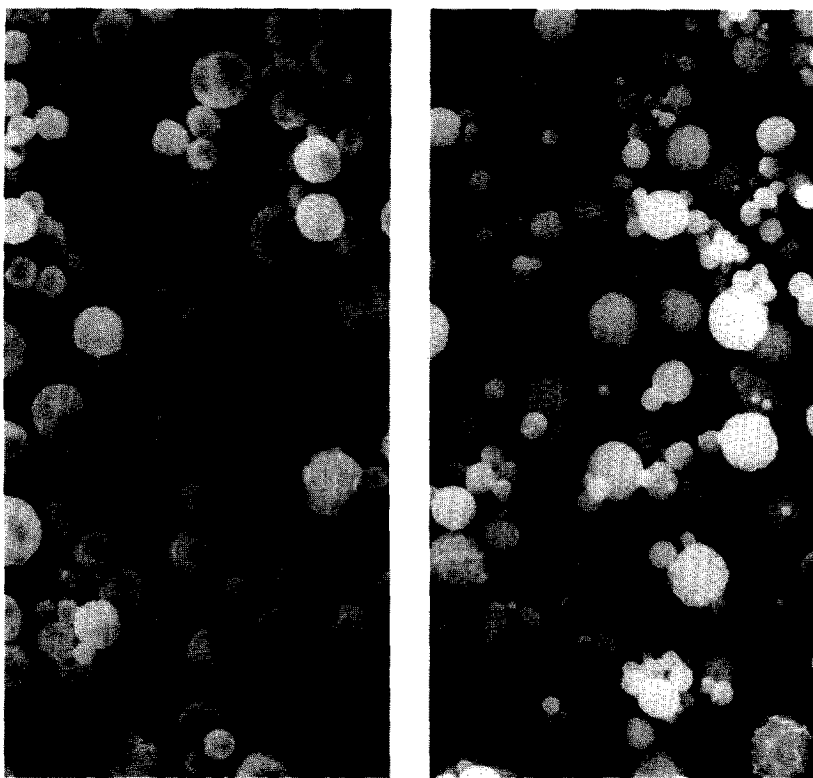


FIG. 3. Scanning electron micrograms of catalysts. Magnification = 5500, (left) aluminum content = 10 at.%, (right) aluminum content = 50 at.%

lative outer surface area of  $1.73 \text{ m}^2/\text{g}$ . The comparison with the BET surface area ( $1.93 \text{ m}^2/\text{g}$ ) suggests that the particles are nonporous.

The catalytic activities for the oxidative coupling of methane were measured on these catalysts. Figure 4 shows the result obtained with the catalyst containing 10 at.% of aluminum. The formation of ethane was observed at temperatures higher than 813 K. Ethylene was not detected at 813 K, but it was formed at higher temperatures. The ethylene/ethane ratio increased with increasing temperature. Other reaction products were carbon monoxide, carbon dioxide, hydrogen, and water. At temperatures higher than 813 K, the rate of formation of carbon dioxide remained almost constant, and the rates of formation of  $\text{C}_2$  hydrocarbons were increased with increasing temperature.

$\text{C}_2$  activity (R2) and  $\text{C}_2$  selectivity (S2) were calculated with these data and are shown as a function of temperature in Fig. 5 together with the total rate of reaction of methane (RT). We shall refer to  $\text{C}_2$  activity as micromoles of  $\text{C}_2$  hydrocarbons formed per unit time per unit surface area of the

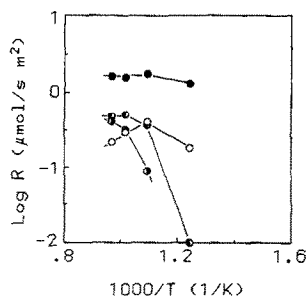


FIG. 4. Effect of reaction temperature. Aluminum content of catalyst = 10 at.%. ○: CO; ●: CO₂; ○●: C=C; ●●: C-C.

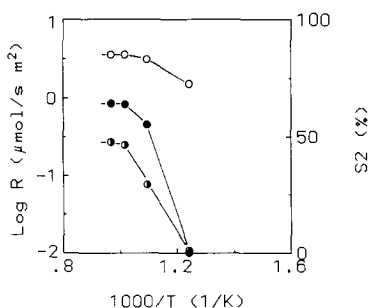


FIG. 5. Total rate,  $C_2$  activity, and  $C_2$  selectivity. Aluminum content of catalyst = 10 at.%.  $\circ$ : RT;  $\bullet$ : R2;  $\bullet$ : S2.

catalyst and  $C_2$  selectivity as the percentage of carbon atoms converted into  $C_2$  hydrocarbons in the total converted methane molecules. The  $C_2$  selectivity increased with increasing temperature, up to 47.9% at 1033 K. A total methane conversion of 25.1%, total oxygen conversion of 95.5%, and  $C_2$  selectivity of 46.8% was observed at 983 K.

Hydrogen was observed in the exit gas in the temperature range (813–1033 K) studied. Thus, at 983 K, the composition (mol%) of the exit gas was as follows: methane (38.1), oxygen (0.47), carbon monoxide (1.05), carbon dioxide (5.73), ethane (1.84), ethylene (1.15), hydrogen (3.97), water (8.05), and nitrogen (39.7). The presence of hydrogen as well as oxygen balance suggests that steam reforming of methane and/or hydrogen forming reactions from methane and oxygen are taking place on the catalyst.

Activities and selectivities for  $C_2$  hydrocarbon formation of various catalysts were compared at 983 K, as shown in Fig. 6. The  $C_2$  activity was increased with increasing aluminum content, showing a maximum at the aluminum content of 10 at.%. The activity decreased only a little in the range between 10 and 50 at.%, but it decreased very much in the range over 50 at.% with a further increase in the aluminum content. The  $C_2$  selectivity remained almost constant in the range between 0 and 50 at.%,

but decreased with a further increase in aluminum content.

Effect of pretreatment temperature was studied with  $LaAlO_3$ . The catalyst was pretreated for 16 h at temperatures between 983 and 1373 K, and changes in catalytic activity and X-ray structure (XRD peak height of  $LaAlO_3$  perovskite (110) plane) was studied. The surface area of the catalyst did not change very much during these pretreatments; the surface area was increased slightly from 1.93  $m^2/g$  at 983 K to 2.40  $m^2/g$  after the pretreatment at 1373 K. An examination with the scanning electron microscope indicated that some cracking of the particles occurred after the high temperature treatment. The pretreatment at higher temperature accelerated the growth of crystalline perovskite phase and decreased the rates of ethane and ethylene formation, as shown in Fig. 7. The ethylene/ethane ratio (from 0.72 to 0.35) and  $C_2$  selectivity (from 48.4 to 36.8%) decreased with increasing pretreatment temperature. This indicates that the active sites for  $C_2$  formation are formed in the amorphous phase.

Figure 8 shows the XRD spectra of a series of catalysts pretreated for 16 h at 983 K. The figure also shows the spectrum of  $La_2O_3$  pretreated at 1473 K for 1 h in the stream of helium. The samples pretreated at 983 K were almost amorphous, and the degree of crystallization was decreased with increasing aluminum content.

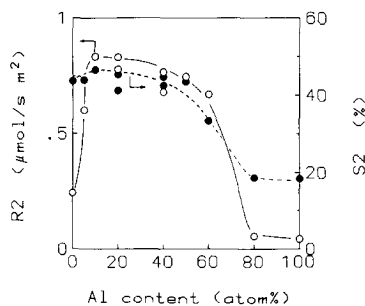


FIG. 6. Effect of aluminum content. Reaction temperature = 983 K.  $\circ$ : R2;  $\bullet$ : S2.

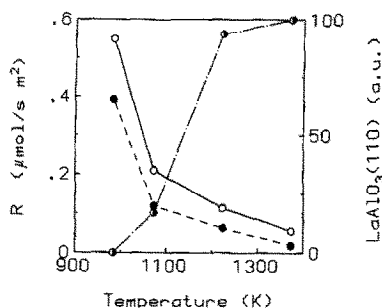


Fig. 7. Effect of pretreatment temperature. Aluminum content of catalyst = 50 at.%, reaction temperature = 983 K. ○: R(C-C); ●: R(C=C); ○:  $\text{LaAlO}_3$  (110) peak height.

The sesquioxide of lanthanum exhibits a characteristic polymorphism and can exist in one or more of three distinct crystalline modifications (hexagonal, monoclinic, and cubic). Standard XRD spectra of these crystals were obtained from the ASTM cards for powder X-ray diffraction spectra, and are shown in Fig. 9. In the sample prepared at 1073 K, or in the present case, the hexagonal structure is stable (19). Figure 8 shows that the stable phase of hexagonal structure was not produced in the pretreatment of 983 K, although it was produced in the pretreatment at 1473 K. The figure also indicates the increase of aluminum content stabilizes the metastable cubic  $\text{La}_2\text{O}_3$  phase.

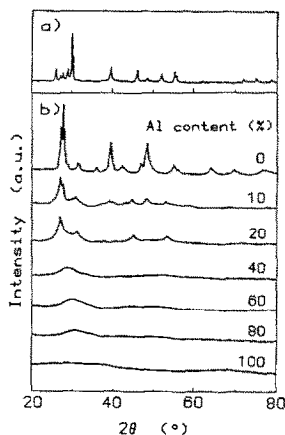


Fig. 8. XRD spectra. (a)  $\text{La}_2\text{O}_3$  pretreated at 1473 K for 1 h. (b) Pretreated at 983 K for 16 h.

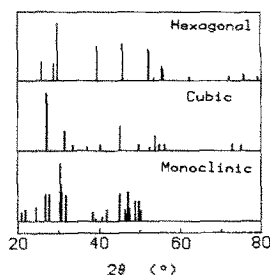


Fig. 9. XRD spectra of  $\text{La}_2\text{O}_3$ .

This fact may be interpreted by the stabilizing effect of the surrounding amorphous phase. If the local structure of the amorphous phase is similar to the crystal structure of the cubic  $\text{La}_2\text{O}_3$ , the interfacial energy between the crystallite and the amorphous phase is diminished and the crystallites of cubic structure are stabilized. In the cubic  $\text{La}_2\text{O}_3$ , cations are octahedrally coordinated, while oxygen anions are tetrahedrally coordinated. The consequence of the above discussion suggests that the local structure of the active amorphous phase is similar to the cubic structure of  $\text{La}_2\text{O}_3$ .

Figure 10 shows the IR spectra of a series of the catalysts. Two absorption bands were appeared at 340 and 730  $\text{cm}^{-1}$  when 10 at.% of aluminum were added into lanthanum oxide. The absorption band of the lower frequency shifted to the higher frequency side and began to decrease at 50 at.% with increasing aluminum content. On the other hand, the absorption band of the higher frequency shifted to the higher frequency side and increased with increasing aluminum content. It should be noted that these bands are quite different from those assigned to crystalline perovskite (20), because sharp absorption bands were developed at 482 and 658  $\text{cm}^{-1}$  with the growth of the perovskite phase after the heat treatment at temperatures higher than 1073 K.

It is well known that the cation-oxygen vibrational frequencies of a coordinated group  $\text{AO}_n$  depend on the coordination

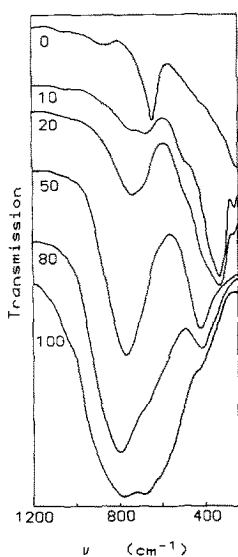


FIG. 10. IR spectra. The aluminum content (at.%) is described in the figure.

number of the cation. In aluminum-containing oxides (21), the characteristic absorption band of  $\text{AlO}_6$  is observed at  $530\text{--}400\text{ cm}^{-1}$  while that of  $\text{AlO}_4$  is observed at  $800\text{--}650\text{ cm}^{-1}$ . Both of these bands shift to the higher frequency side when the coordinated groups are in the condensed phase. The results in Fig. 10 show that the aluminum ions of isolated  $\text{AlO}_6$  are initially produced with the addition of aluminum. This is consistent with the suggestion based on the X-ray analysis. As the aluminum content is increased, the condensation of the isolated  $\text{AlO}_6$  occurs below 50 at.%, but the concentration of the  $\text{AlO}_6$  decreases above 50 at.%. The comparison of these results with those shown in Fig. 6 suggests that the isolated  $\text{AlO}_6$  dispersed in an amorphous lanthanum oxide constitutes the active sites of  $\text{C}_2$  formation.

TPD spectra of the series of catalysts are shown in Fig. 11. A desorption peak of oxygen was observed at 563 K in  $\text{La}_2\text{O}_3$ , while no desorption peak was observed below 920 K in  $\text{Al}_2\text{O}_3$ . In the mixed oxides, two desorption peaks of oxygen were observed below 980 K. The lower temperature peak showed a maximum at about 20

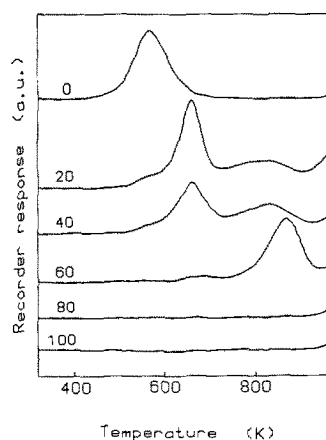


FIG. 11. TPD spectra. The aluminum content (at.%) is described in the figure.

at.% with increasing aluminum content. On the other hand, the higher temperature peak showed a maximum at about 60 at.%. These desorption peaks were decreased when the sample was treated at 1373 K for 16 h, as shown in Fig. 12. The amounts of oxygen molecules desorbed from the  $\text{LaAlO}_3$ , pretreated at 983 K, were 1.5 and  $3.4\text{ }\mu\text{mol/m}^2$ , respectively, for lower temperature and higher temperature peaks. As the monolayer coverage of oxygen is  $11\text{ }\mu\text{mol/m}^2$ , these sites may be composed of a special lanthanum aluminum combination on the surface. These facts indicate that these sites are characteristic of the active amorphous materials and suggest that these sites are responsible for the  $\text{C}_2$  hydrocarbon formation.

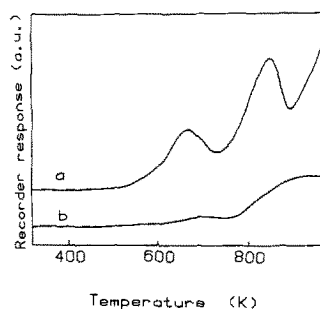


FIG. 12. TPD spectra of  $\text{LaAlO}_3$ . (a) Pretreated at 983 K for 16 h. (b) Pretreated at 1373 K for 16 h.

## REFERENCES

1. Mitchell, H. L., and Waghorne, R. H., U.S. Patent 4172810 (1979); 4239658 (1980).
2. Keller, G. E., and Bhasin, M. M., *J. Catal.* **73**, 9 (1982).
3. Hinsén, W., and Baerns, M., *Chem.-Ztg.* **107**, 223 (1983).
4. Hinsén, W., Bytyn, W., and Baerns, M., "Proceedings, 8th International Congress on Catalysis, Berlin, 1984," Vol. 3, p. 581. Dechema, Frankfurt-am-Main, 1984.
5. Ito, T., and Lunsford, J. H., *Nature (London)* **314**, 721 (1985).
6. Otsuka, K., Jinno, K., and Morikawa, A., *Chem. Lett.*, 499 (1985).
7. Garcia, E. Y., Rivera, G. L., and Resasco, D. E., *React. Kinet. Catal. Lett.* **28**, 431 (1985).
8. Ito, T., Wang, J., Lin, C., and Lunsford, J. H., *J. Amer. Chem. Soc.* **107**, 5062 (1985).
9. Imai, H., and Tagawa, T., *J. Chem. Soc., Chem. Commun.*, 52 (1986).
10. Lin, C., Cambell, K. D., Wang, J., and Lunsford, J. H., *J. Phys. Chem.* **90**, 534 (1986).
11. Otsuka, K., Liu, O., Hatano, M., and Morikawa, A., *Chem. Lett.*, 467 (1986).
12. Otsuka, K., Liu, O., and Morikawa, A., *J. Chem. Soc., Chem. Commun.*, 586 (1986).
13. Otsuka, K., Jinno, K., and Morikawa, A., *J. Catal.* **100**, 353 (1986).
14. Emesh, I. T. A., and Amenomiya, Y., *J. Phys. Chem.* **90**, 4785 (1986).
15. Aika, K., Moriyama, T., Takasaki, N., and Iwamatsu, E., *J. Chem. Soc., Chem. Commun.*, 1210 (1986).
16. Asami, K., Hashimoto, S., Shikada, T., Fujimoto, K., and Tominaga, H., *Chem. Lett.*, 1233 (1986).
17. Imai, H., and Orito, H., *Nippon Kagaku Kaishi*, 851 (1984).
18. Imai, H., Takami, K., and Naito, M., *Mater. Res. Bull.* **19**, 1293 (1984).
19. Topp, N. E., "Chemistry of the Rare-Earth Element," Elsevier, New York, 1965.
20. Couzi, M., and Houng, P. V., *J. Chim. Phys. Phys.-Chim. Biol.* **69**, 1339 (1972).
21. Tarte, P., "Proc. Intern. Conf. Physics of Non-Crystalline Solids," p. 549 (1965).